Supplemental Materials

Molecular Biology of the Cell

Mehrotra et al.

SUPPLEMENTAL INFORMATION

Alternate pleckstrin homology domain orientations regulate dynamin-catalyzed membrane fission

Niharika Mehrotra, Justin Nichols and Rajesh Ramachandran*

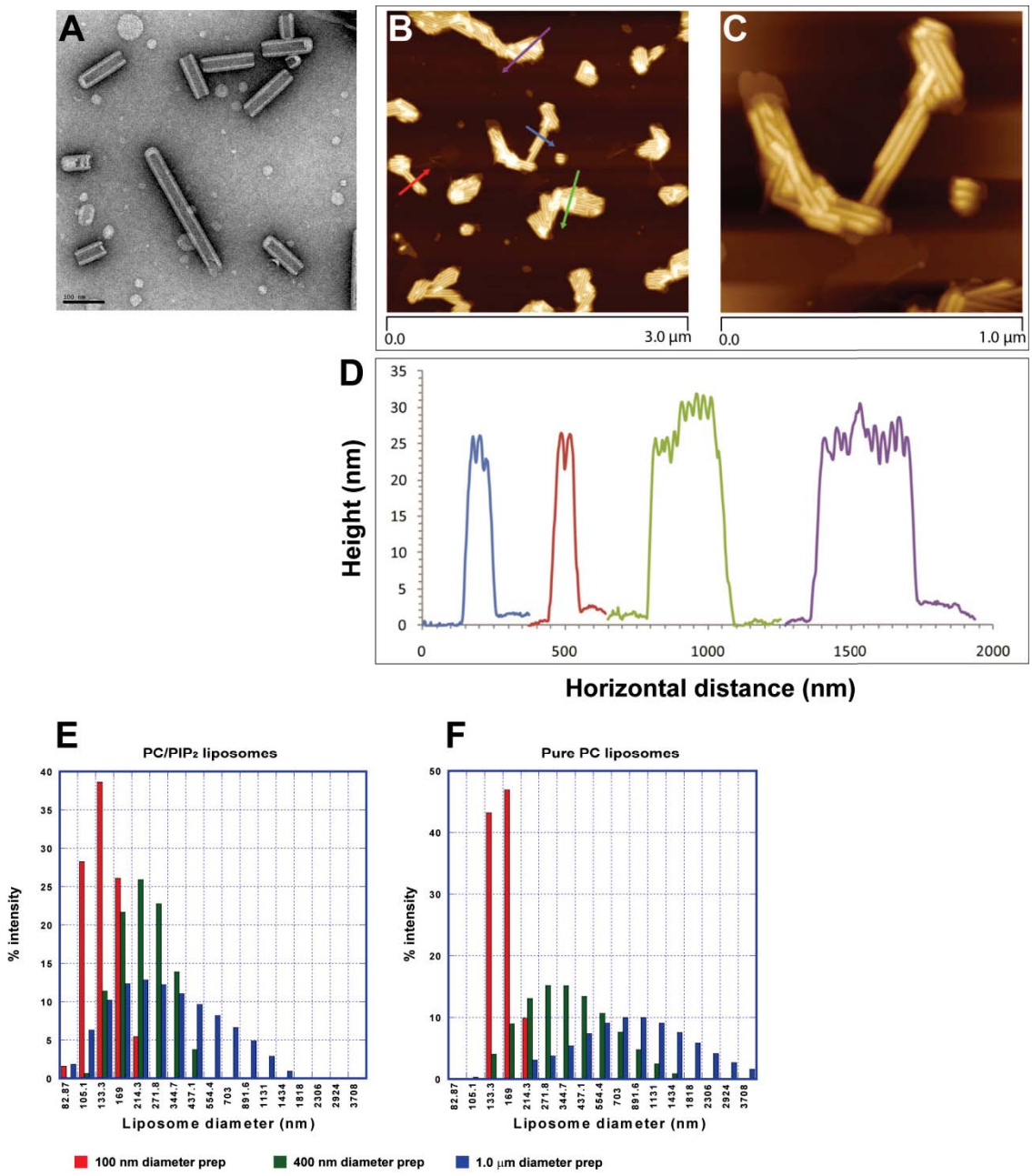

Figure S1. EM, AFM and DLS measurements of lipid template diameter and size distribution. (**A**) Negative-stain EM of LT showing homogeneity of cross-sectional diameter (Scale bar: 100 nm) (**B**) A representative AFM image of nanotubes showing a 3 x 3 µm scanning region. LT tended to cluster on the mica surface upon drying. (**C**) A finer 1 x 1 µm AFM scan shows finer features of LT at the center of the image in panel A. (**D**) The cross-sectional profiles of LT are colored accordingly to match reference lines in panel B. The profiles show that the LT are of nearly uniform diameter; their cross-sectional heights are between 25-30 nm. (**E** and **F**) Representative DLS data for the size distribution of liposomes prepared by extrusion through 100-, 400- and 1000-nm pore diameter polycarbonate membranes. The % intensity contribution from each diameter species is plotted as a histogram. In comparison to pure DOPC liposomes (**F**), 10 mol% PIP_2-containing liposomes (left panels) extruded through 400- and 1000-nm pore diameter membranes tended to generally smaller.

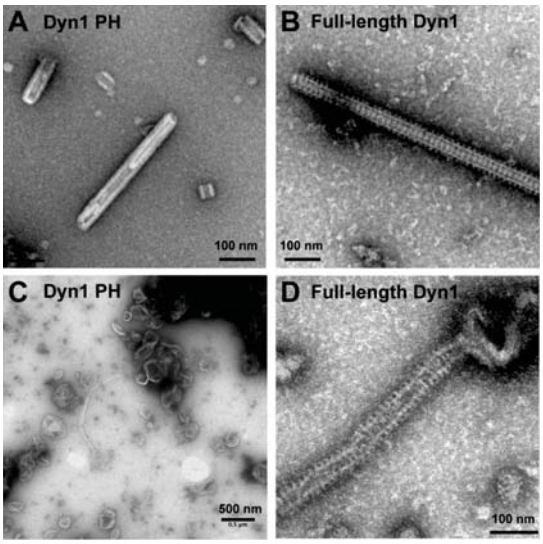

Figure S2. Negative-stain EM of Dyn1PH WT and full-length Dyn1 WT on LT (**A** and **B**) and 400 nm diameter liposomes (**C** and **D**), respectively. Representative images are shown. Samples were deposited on carbon-coated grids and visualized as described under Methods.

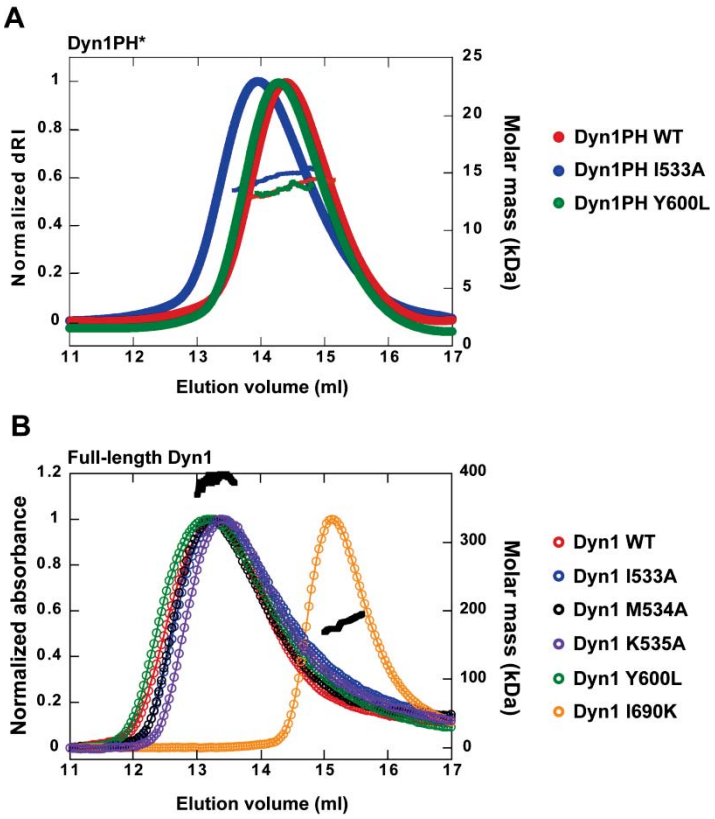

Figure S3. SEC-MALS analyses of Dyn1PH and full-length Dyn1 mutants. (**A**) Isolated Dyn1PH WT and mutants were sieved on a Superdex 75 10/300 GL size-exclusion column and analyzed online by MALS as described under Methods. MALS analyses revealed a monodisperse population of monomers of ~14 kDa for all species (horizontal traces). (**B**) Full-length dynamin variants were analyzed likewise using a Superose 6 10/300 GL column. All PH domain mutants of full-length dynamin examined in this study formed stable WT-like tetramers of ~400 kDa in contrast to the ~200 kDa dimers formed by the Dyn1 I690K GED mutant.

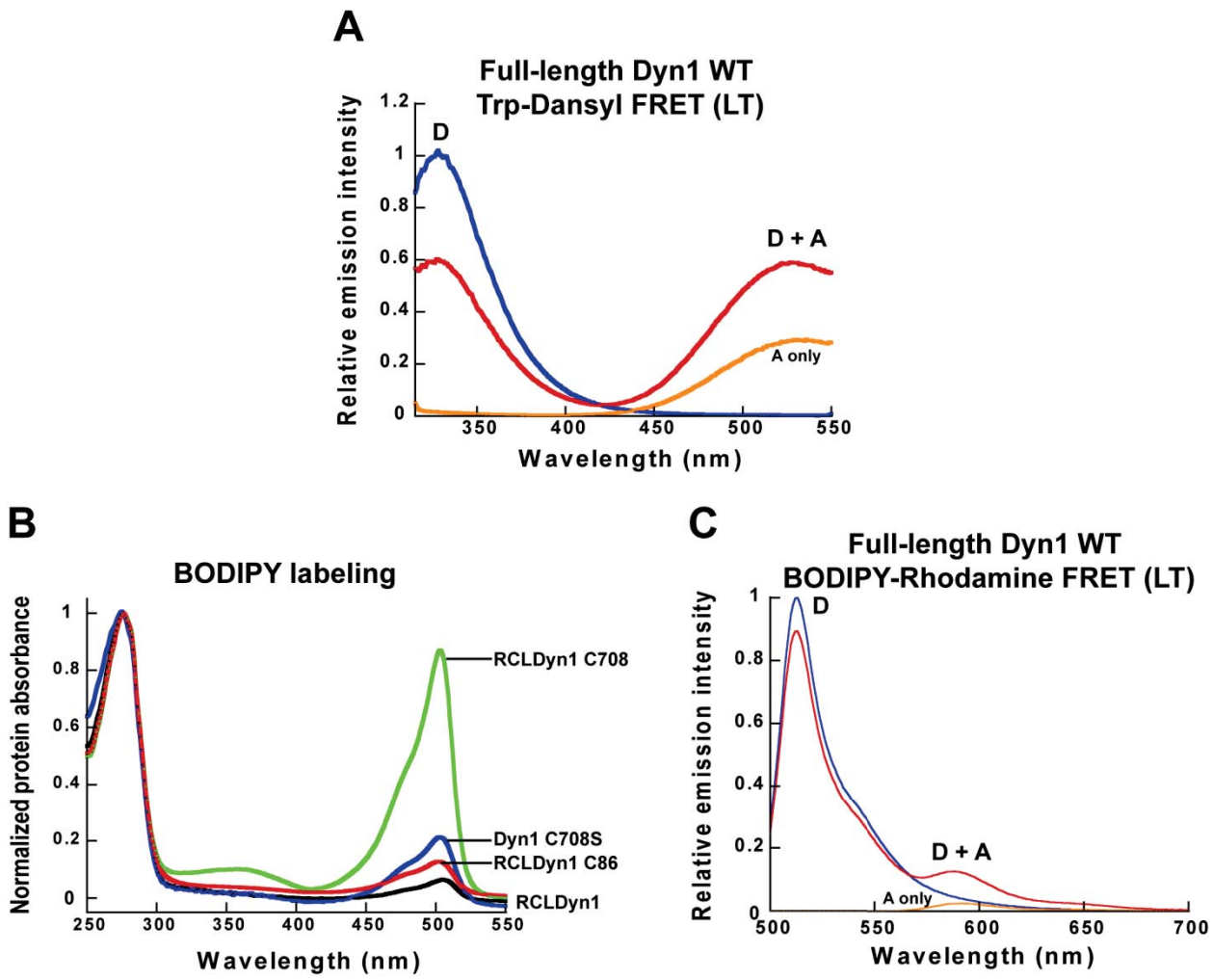

Figure S4. Demonstration of Trp-Dansyl and BODIPY-Rhodamine FRET. (**A**) Representative Trp-Dansyl emission spectra of samples containing: Dyn1 WT (**D**onor only; BLUE) in the presence of unlabeled LT; Dyn1 WT in the presence of Dansyl-labeled LT (**D**onor plus **A**cceptor; RED); and Dansyl-labeled LT (**A**cceptor only sample; ORANGE) in the absence of protein. FRET was ascertained by the donor emission intensity decrease at 330 nm and sensitized acceptor emission intensity increase at 530 nm upon donor excitation (λ_{ex} = 280 nm). The protein and lipid concentrations were 0.1 μM and 5 μM, respectively. LT contained 10 mol% PIP_2. (**B**) Identification of native C708 in GED as the primary target of BODIPY labeling in Dyn1. Normalized absorption spectra of BODIPY-labeled RCLDyn1 C708 (GREEN) and RCLDyn1 C86 (RED) in which all other native Cys residues have been substituted with Ser (**R**eactive **C**ys-**l**ess Dyn1; Ramachandran and Schmid, 2008) relative to Dyn1 C708S (BLUE) and RCLDyn1 (BLACK; background labeling in the absence of native Cys residues) (Ramachandran et al., 2007, Ramachandran and Schmid, 2008). The efficiency of labeling was ~70-80% for RCLDyn1 C708 and ~20-30% for Dyn1 C708S (WT background) adding up to the 1:1 labeling achieved for Dyn1 WT and mutants. (**C**) Representative BODIPY-Rhodamine emission spectra of biochemically equivalent samples containing: BODIPY-Dyn1 WT (**D**onor only; BLUE) in the presence of unlabeled LT; BODIPY-Dyn1 WT in the presence of RhPE-labeled LT (**D**onor plus **A**cceptor; RED); and RhPE-labeled LT (**A**cceptor only sample; ORANGE) in the presence of unlabeled Dyn1 WT. FRET was ascertained by the donor emission intensity decrease at 510 nm and sensitized acceptor emission intensity increase at 590 nm upon donor excitation (λ_{ex} = 470 nm). The protein and lipid concentrations were 0.1 μM and 5 μM, respectively. LT contained 10 mol% PIP_2.

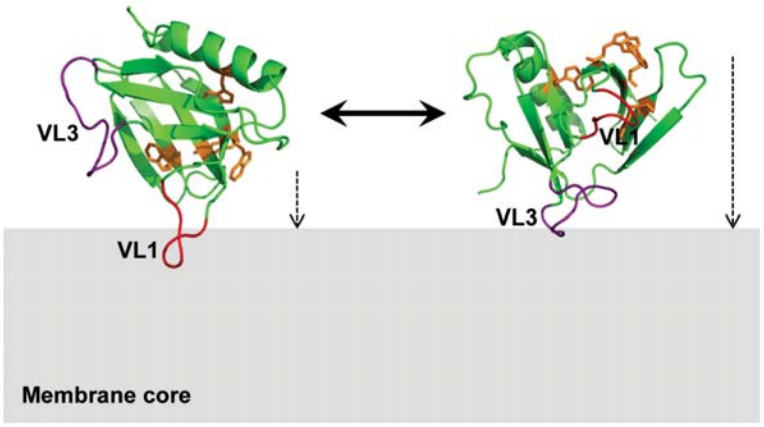

Figure S5. Alternate orientations of the Dyn1 PH domain (PDB ID: 1DYN) that position either VL1 or VL3 proximally to the membrane surface. Dashed arrows represent the change in distance between the Trp cluster and the membrane surface between the two orientations.

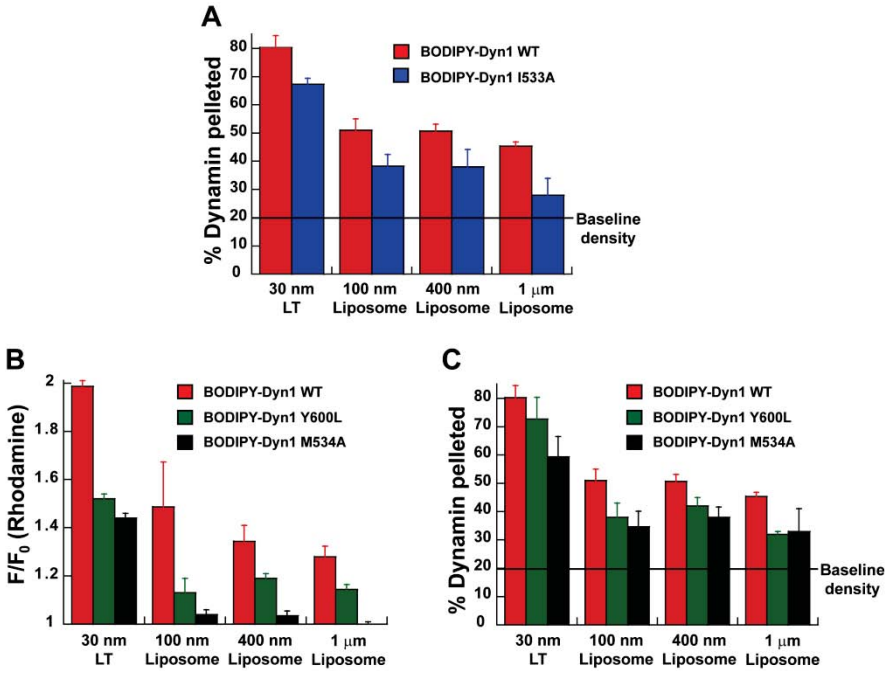

Figure S6. Spin-sedimentation profiles for BODIPY-labeled full-length Dyn1 mutants and measurement of BODIPY-Rhodamine FRET in Dyn1 Y600L and Dyn1 M534A. (**A**) Stable binding of BODIPY-labeled-Dyn1 WT or -Dyn1 I533A (2.0 μM) to lipid templates of varying membrane curvature (100 μM total lipid) was examined by spin-sedimentation followed by SDS-PAGE and densitometric analyses of the supernatant (S) and pellet (P) fractions as described under Methods. % dynamin pelleted with the various templates is plotted. (**B**) FRET-sensitized increase in Rhodamine emission intensity upon incubation of lipid templates of varying membrane curvature containing 1 mol% RhPE (5 μM total lipid) with either BODIPY-labeled-Dyn1 Y600L or -Dyn1 M534A (0.1 μM) relative to BODIPY-labeled-Dyn1 WT monitored at 590 nm and plotted as F/F_0. F_0 is the background emission intensity of Rhodamine (by direct excitation at λ_{ex} = 470 nm) at time '0' prior to protein addition, and F, the intensity after 15 min of protein incubation. (**C**) Same as in panel (A) but with data for BODIPY-labeled-Dyn1 Y600L and -Dyn1 M534A plotted relative to BODIPY-labeled-Dyn1 WT.

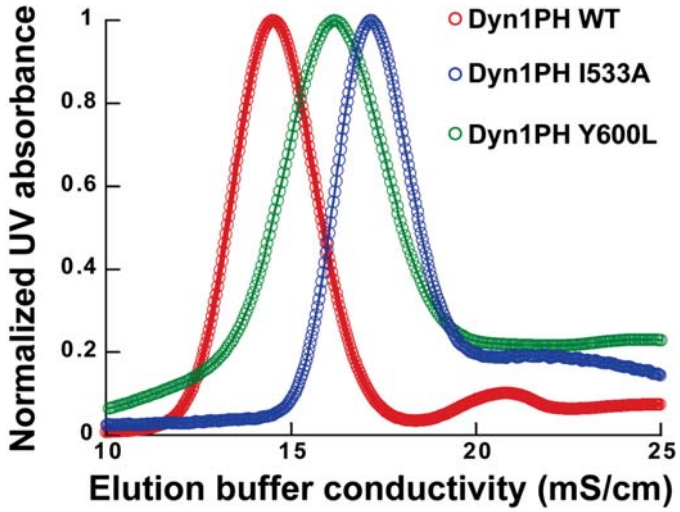

Figure S7. Mixed population of PH domain orientations in Dyn1PH Y600L. Same as in Fig. 5C. but with the inclusion of data for Dyn1PH Y600L.

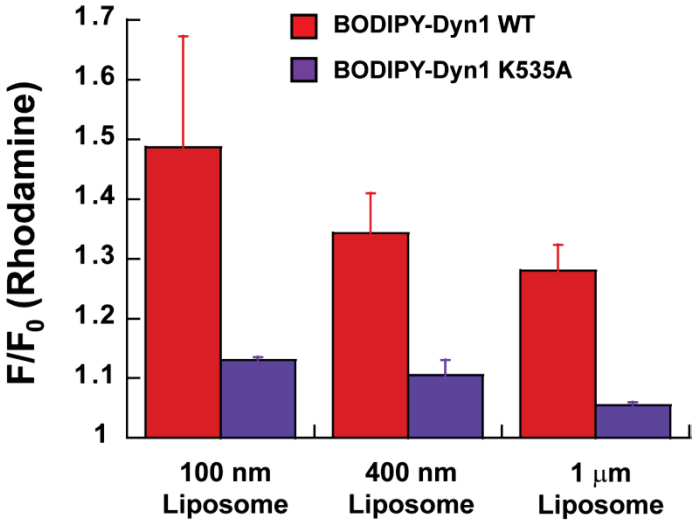

Figure S8. Comparison of BODIPY-Rhodamine FRET in BODIPY-Dyn1 WT and BODIPY-Dyn1 K535A. Same as in Fig. S6B but with the inclusion of data for BODIPY-Dyn1 K535A.